Article:

Kalliomäki, H, Torvela, TM, Moreau, J et al. (1 more author) (2014) Relationships between basin architecture, basin closure, and occurrence of sulphide-bearing schists: an example from Tampere Schist Belt, Finland. Journal of the Geological Society, 171 (5). 659 - 671. ISSN 0016-7649

https://doi.org/10.1144/jgs2013-122

Relationships between basin architecture, basin closure, and occurrence of sulphide-bearing schists: an example from Tampere Schist Belt, Finland

H. Kalliomäki[1], T. Torvela[2,*], J. Moreau[3] & Y. Kähkönen[1]

[1)] University of Helsinki, Department of Geosciences and Geography, PO Box 64, FI-00014 University of Helsinki, Finland

[2)] University of Leeds, School of Earth and Environment, Leeds, LS2 9JT, UK

[3)] University of Copenhagen, Department of Geography and Geology, Øster Voldgade10, 1350 Copenhagen, Denmark

* Corresponding author, email (T. Torvela) *t.m.torvela@leeds.ac.uk*

Abstract

We present field observations from the Palaeoproterozoic volcano-sedimentary Tampere palaeobasin, where the primary structures have been exceptionally well preserved. We use the observations to construct a new tectonic model for the southeastern margin of the Tampere basin during its inversion and subsequent closure. The observed volcano-sedimentary and structural features suggest a change in the local structural style from thick-skinned inversion to thin-skinned thrusting, in order to accommodate the crustal shortening during basin closure. Furthermore, it is suggested that there is a genetic relationship between the interpreted palaeothrusts and the sulphide-bearing schist horizons in the study area. On a more general note, the results infer that presently subvertical mineralised shear zones may have originally been gently dipping, further suggesting that the mineralised fluids may not necessarily have been sourced from great depths (i.e. from deep within the basement).

Introduction

Ancient basins archive the early development of plate tectonics, life, and ore-bearing systems. Especially basins involving volcanic-derived materials contain economically important ore and mineral deposits (e.g. Lentz 1998; Weihed *et al*. 2005). The formation of these ores is often related to hydrothermal activity and the migration of mineralising fluids: this can happen both in locally extensional environments (notably the formation of the volcanogenic massive sulphide deposits, 'VMS ores', which most commonly form in volcanic arc settings; e.g. Ohmoto 1996; Allen *et al*. 2002) but mineralising fluids can also move along strike-slip or reverse faults (e.g. Sibson *et al*. 1988; Teagle *et al*. 1990; Piessens *et al*. 2002). Usually the mineralisations formed in compressional settings are related to steep strike-slip or reverse faults where the fluids are sourced from great depths; reported mineralisations related to more gently dipping reverse faults are less common (e.g. Nguyen *et al*. 1998; Piessens *et al*. 2002).

The Tampere Schist Belt (TSB) in southern Finland is a c. 1.92-1.88 Ga volcano-sedimentary basin that underwent inversion and closure between c. 1.89-1.88 Ga (Fig. 1; Patchett & Kouvo 1986; Kähkönen *et al*. 1989; Nironen 1989a; Rutland *et al*. 2004). The tectonic setting of the belt varied with time from a microcontinental rift to a volcanic arc system (Lahtinen et al., 2009). The closure of the basin resulted in the formation of a large-scale, predominantly tight to isoclinal syncline with steeply dipping fold axial planes (Figs. 1b & 2; e.g. Kähkönen 1989; Nironen 1989a). Despite the crustal-scale shortening, the primary sedimentary and volcanic structures are generally remarkably well preserved. The TSB, therefore, offers an excellent opportunity to examine the volcano-sedimentary evolution of an ancient basin, and the mechanics of and strain distribution during its subsequent closure. In addition, the TSB is valuable for understanding the evolution of ore-bearing systems within volcano-sedimentary basins as it hosts several mineralised deposits. Probably the best known of these are the Haveri deposit, mined in 1942-1962, and the presently mined Kutemajärvi deposit (Fig. 1b). The Haveri Fm. forms the base of the TSB succession and hosts an orogenic gold deposit (originally a VMS ore that was later remobilised; Nironen 1994; Eilu *et al*. 2003). The Haveri deposit is hosted by schists and is associated with faults and folds (Nironen 1994). Various sulphide-bearing schist horizons and lenses are also contained higher in the local stratigraphy (e.g. Kähkönen & Nironen 1994). The Kutemajärvi deposit is interpreted to be an epithermal ("shallow heat") metamorphic deposit (Eilu *et al*. 2003). It, too, is associated with schists and prominent fault zones (Poutiainen & Grönholm 1996).

The aim of this study is to investigate the structural development and the architecture of a part of the TSB in more detail, including the relationships between the volcano-sedimentary sequences, the tectonic structures, and the sulphide-bearing schist horizons. Important insights are gained into understanding the mechanisms of the basin closure and the localisation of the sulphide mineralisation within the basin. The suggested conceptual model implies that early, gently dipping thrusts acted as both channels and traps for the mineralising fluids that possibly sourced either locally or from relatively shallow depths from the base of the basin infill. The continued compression caused a subsequent rotation of the thrusts into their present subvertical position. Although the studied rocks have been somewhat metamorphosed, we have in general dropped out the prefix "meta" from rock type names.

Geological setting

The continental crust of the central Fennoscandian Shield is mainly composed of 1.95-1.80 Ga rocks, forming the so-called Svecofennian domain (Fig. 1a; Gaál & Gorbatschev 1987). The orogenic evolution that produced this orogen was considered as the single Svecofennian orogeny by Gaál & Gorbatschev (1987), while Lahtinen *et al*. (2005) divided it into three separate orogenies: the Fennian arc-accretionary orogeny at c. 2.0-1.85 Ga, the Andean-type Svecobaltic orogeny at c. 1.84-1.80 Ga, and the Nordic orogeny with a continent-continent collision at 1.82-1.79 Ga (Fig. 1a; Lahtinen *et al*. 2005). Rutland *et al*. (2004) and Williams *et al*. (2008) divide the earliest orogeny ('Fennian' in Lahtinen *et al*. 2005) into two orogenic episodes; the Early Svecofennian orogeny (or 'pre-Bothnian) before c. 1.92 Ga, and a Middle Svecofennian orogeny (or 'post-Bothnian') at c. 1.88-1.85 Ga. The two events were separated by rifting/extension of the pre-Bothnian basement and associated volcano-sedimentary deposition. They also conclude that the pre-Bothnian rocks were deposited in a large marginal basin and that neither the pre-Bothnian nor the post-Bothnian events were arc-accretionary. In any case, most of the igneous and sedimentary rocks in central and southern Finland formed during the early "Fennian" event(s), before c. 1.85 Ga (e.g. Lahtinen *et al.* 2005, and references therein).

The E-W striking Tampere Schist Belt (TSB) lies in the centre of the Svecofennian domain (Fig. 1). The entire TSB is c. 200 km long (Fig. 1a) but its best studied central part, from Viljakkala in the west to Orivesi in the east, extends for about 60 km (Fig. 1b). In the north, the TSB is bounded by the igneous rocks of the c. 1.88 Ga Central Finland Granitoid Complex CFGC (e.g. Nironen *et al.* 2000). To the south of the TSB lies the Vammala migmatite belt VMB (also known as the Pirkanmaa belt). The TSB – VMB contact is strongly sheared along the curvilinear "Tampere shear zone" (TSZ), and intruded by the c. 1.88-1.87 Ga Siitama batholith near Orijärvi (Figs. 1b & 2; Nironen *et al.* 2000). The batholith is internally relatively undeformed but is clearly sheared along the assumed continuation of the TSZ.

The TSB is characterised by 1.90-1.89 Ga metavolcanic and related sedimentary rocks with volcanic arc -type geochemistries, and by turbiditic metasedimentary rocks originally deposited between c. 1.92-1.90 Ga (e.g. Seitsaari 1951; Ojakangas 1986; Kähkönen 1987, 1989; Lahtinen *et al.* 2009). The rocks are metamorphosed in low-T amphibolite to transitional greenschist/amphibolite facies conditions (Kilpeläinen *et al.* 1994). Overall, the central TSB defines a main syncline with an E-W striking, subhorizontal hinge zone and a steeply dipping axial plane (Figs. 1b & 2; Seitsaari 1951; Kähkönen 1989; Nironen 1989). The northern limb is dominated by volcanic rocks, while the southern limb is considerably richer in sedimentary rocks, although towards the southernmost margin volcanics again become more abundant (e.g. Seitsaari 1951; Kähkönen 1994, 1999).

The nature of the basement underlying the TSB volcanics and sediments is unknown, but Lahtinen & Huhma (1997) imply that evolved crust and associated mantle were in place in the area around the onset of the extension at c. 1.92 Ga. The lowermost recognised syn-rift unit is the volcanic Haveri Formation in the central TSB, and it consists of (proto)oceanic crust (Fig. 1b; Mäkelä 1980; Kähkönen & Nironen 1994; Kähkönen 2005; Lahtinen *et al.* 2009). The lower part of the Haveri Fm. is characterized by pillow lavas with enriched mid-oceanic ridge/within plate basalt (EMORB/WPB) geochemistry. The upper part consists of cherts, sedimentary carbonates, and black schists. The Haveri Fm. is overlain by the sedimentary Osara Formation, equivalent to the Myllyniemi Formation near Lake Näsijärvi. These formations consist mostly of what are in the TSB literature often referred to as "turbidites"; greywackes and pelites deposited in submarine fan channels with dominantly westerly palaeocurrents (Fig. 1b; Mäkelä 1980; Ojakangas 1986; Kähkönen 1989). The Myllyniemi Fm resembles the sedimentary rocks at Karppi, Orivesi in the east and are considered to represent the same unit (Fig. 1b; e.g. Seitsaari 1951).

Sulphide-bearing schist layers are found locally within the lower parts of the Myllyniemi Fm, including the Karppi area. Upwards in the TSB succession, the Myllyniemi sediments and their lateral counterparts are overlain by subduction-related basaltic to rhyolitic volcanic rocks and by conglomeratic to pelitic sedimentary rocks derived thereof (Fig. 2; Seitsaari 1951; Simonen 1953; Kähkönen 1999).

The Myllyniemi-type sediments were deposited between 1.92-1.90 Ga. The maximum age of deposition is constrained by detrital zircons in the Osara and Myllyniemi Fms (minimum U-Pb ages of c. 1.92 Ga; Huhma *et al*. 1991; Claesson *et al*. 1993; Lahtinen *et al*. 2009). The minimum age of deposition is given by the 1898±8 Ma age for the volcanic unit at Pirttiniemi, stratigraphically directly overlaying the Myllyniemi Fm (Kähkönen 1989; Kähkönen *et al*. 2004). In addition, the volcanics-dominated unit along the southern margin of the TSB, the "Tohloppi-Kiviranta-Sorila volcanics" have been dated at 1892±2 Ga (magmatic age from a dacite at Tesoma close to Tohloppi; Kähkönen 1994; Kähkönen *et al*., 2004). Despite their apparent position below the Myllyniemi Fm on the map (Fig. 1b), the Tohloppi volcanics are, therefore, also younger than the Myllyniemi sediments and might be equivalent with the Pirttiniemi volcanics (Kähkönen 1994). The onset of the basin inversion and the timing of the final closure are not well constrained, but it is implied that the crust was already thickened by c. 1.88 Ga. Two large plutons of approximately this age intrude the TSB: the Värmälä pluton with a U-Pb zircon age of 1878±3 (Nironen 1989b; Figs. 1b & 2), and the Hämeenkyrö pluton, dated at c. 1882±6 Ma (U-Pb zircon age; Fig. 1c; Patchett & Kouvo 1986). Minor extrusive volcanism and related deposition at this stage is, however, also implied (c. 1.88 Ga; Kähkönen & Huhma, 2012).

The relationship between the Vammala Migmatite Belt VMB and the TSB is important in order to understand the tectonic setting of the TSB deposition. The gneisses and migmatites of the VMB are dominated by metasedimentary rocks of interpreted turbiditic origin. Volcanogenic rocks are not common and, where present, mostly show MORB- or WPB-affinities, similar to the Haveri Fm. of TSB, rather than subduction-related characteristics. In addition, the VMB is considerably richer in black schists that the TSB. A relatively deep basin setting for much of the VMB is implied, but sedimentary rocks more typical for shelf and/or upper parts of submarine fan environments have also been found (Lahtinen et al., 2009). The temporal and spatial relationship between the two belts has been controversial. Nironen (1989a) suggested that the TSB and VMB belong to the same unit but possibly represent different crustal levels/metamorphic conditions. Kähkönen (1999, 2005) considered the VMB largely as the subduction zone complex related to the arc volcanism in the TSB. However, age determination results imply that VMB includes pre-1.91 Ga rocks, so that the TSB sediments and volcanics were deposited in a basin formed during extension of this basement (Rutland *et al*. 2004). On the other hand, Lahtinen *et al*. (2009) show that the Myllyniemi-type metasediments in the lower part of the TSB succession and bulk of the VMB turbidites are identical in detrital zircon age populations, and that a part of the VMB sedimentary rocks have c. 1.89 Ga detrital zircon probably derived from the TSB arc volcanics. Lahtinen *et al*. (2009) also emphasized changes in the sedimentary and tectonic environments during evolution of the TSB and VMB. In their model, the basalts and the sedimentary rocks of the Haveri Fm. were formed during rifting of a c. 2.0 Ga microcontinent. As the rifting continued, the sedimentation environment changed to a passive margin, and the Myllyniemi-type sediments were deposited at c. 1.92-1.90 Ga. The onset of subduction and TSB arc-type volcanism at c. 1.90 Ga caused a change from a passive margin/continental slope setting to that of an (intra-)arc system, where the 1.90-1.89 Ga TSB volcanism represent the 'proper' volcanic arc and the VMB acted mainly as the accretionary complex.

The folding that produced the main Tampere syncline is interpreted to be associated with the main basin inversion and closure event (Fig. 2; F_1 folding phase of Nironen 1989a). Especially the southern limb seems to contain several tight to isoclinal, upright F_1 folds with gently dipping to subhorizontal fold axes/hinge lines, 'parasitic' with respect to the main regional syncline (Fig. 2; Nironen 1989a). The southern limb is bounded by the Tampere shear zone: kinematic indicators imply thrusting toward north (i.e. reverse south-side up; Figs. 1b & 2; e.g. Nironen 1989a; Kähkönen 1999). Nironen (1989a) suggests that the displacement along the thrust was essentially vertical, and that the thrust formed during the first deformation phase D_1, i.e. simultaneously with F_1. The strike-slip kinematics of the TSZ are not yet described in the literature; near Tampere, asymmetric structures have not been observed in the horizontal plane (Nironen 1989a). Nironen (1989a) further suggests that the Hämeenkyrö and Värmälä plutons (Figs. 1 & 2) intruded during the F_1.

The area of this study is located in the eastern part of the TSB (Figs. 1 & 2). The area was chosen for two main reasons: i) it represents the (presumably) lower level of the stratigraphy, the tectonic development and the present structural geometry of which is largely unknown; and ii) it contains some sulphide-bearing schist horizons/lenses and geophysical anomalies that are assumed to be associated with the schist horizons. The relationships of the sulphide-bearing schists to the overall volcano-sedimentary architecture and/or the tectonic history are unknown. Kähkönen (1999) identifies two units, Karppi turbidites and Pohjala volcanics, in the area (Figs. 1b, 2). The Karppi turbidites in the north consists of greywackes and mudstones, whereas the Pohjala volcanics in the south contain various volcaniclastic rocks in addition to massive plagioclase- and plagioclase-uralite-porphyrys. The Karppi Fm. has been correlated with the Myllyniemi and Osara Fms. further west (Kähkönen 1999, 2005).

Observations

The exposure in the entire TSB is limited due to gentle topography, widespread Quaternary deposits, and thick soils. However, in more elevated areas, good-quality outcrops are available or can be created with reasonable effort, enabling representative observations. Special attention was paid to the structural and volcano-sedimentary features, the architecture, and the spatial relationships of the mapped rocks.

Like elsewhere within the TSB, the studied supracrustal rocks show well preserved primary structures, despite the evidently considerable shortening during basin closure (Fig. 3). In many places, the S_0 (bedding) top-of-strata indicators and various other primary structures are clearly identifiable. The strata are usually strongly tilted with dips of >70°. The first secondary foliation (local S_1) is a roughly E-W to NEE-SWW striking schistosity, mostly subparallel to S_0 (Fig. 4). A younger secondary schistosity S_2 is seen to strike at an angle to S_1, usually NE-SW and crenulating the S_1 (Fig. 3h). The S_1 and S_2 vary in intensity depending on the rock type: the fine-grained, mica-rich mudstones often show intense schistosity, while the coarser-grained sedimentary and volcanic rocks may seem almost undeformed (Fig. 3). Kinematic markers (sigma clasts, S-C structures) are observed occasionally, mostly in the south. On subhorizontal surfaces, they record both dextral and sinistral sense of shear. However, shearing becomes more intense toward the south and sinistral kinematic markers become dominant close to the implied continuation of the Tampere shear zone.

At least two different folding styles (here called F_1 and F_2) are distinguishable in the field. F_1 shows tight to isoclinal folds with subvertical fold axial planes and gently to moderately (up to c. 40°) plunging fold axes/hinge lines. F_2 is observed in the southern part of the mapping area, where it is seen to refold F_1. F_2 displays open to closed folds with steep axial planes and fold axes plunging c. 60-70° (Fig. 4).

The rock types are here divided into two main lithological units: the metavolcanics-dominated southeastern part (the volcanic unit VU); and the metasiliciclastics-dominated northern part (siliciclastic unit SCU) (Figs. 3 & 4). There is a sharp transition from one unit to the other, only observable in the eastern part of the mapping area due to the c. 1.88-1.87 Ga Siitama batholith intruding the units in the western part (Fig. 4).

The two main units SCU and VU are very distinct and display different lithological, architectural, and structural characteristics. The VU is composed both of coherent porphyritic rocks, evidently lavas, domes, and/or sills in origin, and of stratified volcanic rocks. (Fig. 4). Individual unit thicknesses reach up to c. 150 m. Some sedimentary (volcaniclastic) rocks are found in the central part of the VU. S_1 is usually (sub)parallel to S_0 in the VU, and is best developed in the finer-grained layers. S_1/S_0 normally follows an E-W strike throughout the VU, except at the contact with Siitama batholith. The top-of-strata indicators (graded bedding, erosion surfaces) are common and dominantly towards the south, except in the southern part of the VU where the younging direction is towards the north (Fig. 4). The SCU rocks on the other hand are dominated by sandstones, but pebble conglomerates and mudstones (shales and schists) are common as well. Individual beds within the SCU are of variable thicknesses, from cm-scale to m-scale. Top-of-strata indicators systematically, with one possible exception close to the VU-SCU contact, indicate northward younging directions (ripples, graded bedding, erosion surfaces; Figs. 3g, h). As with the VU, S_1/S_0 mostly follows an E-W strike except locally in the vicinity of the Siitama batholith. S_2 schistosities are commonly observed in mudstones, striking mostly approximately SSW-NNE to WSW-ENE (Figs. 3h & 4).

Based on the southwards-younging pattern of the VU, the stratigraphic succession of the VU subunits can be defined (from bottom to top): (VU1) felsic volcaniclastics, (VU2) intermediate volcaniclastics, (VU3) coherent felsic plagioclase porphyrys, (VU4) coherent uralite-plagioclase (ur-pl) porphyritic rocks (lavas or sills), (VU5) volcaniclastics including conglomerates and sandstones (here called “southern volcaniclastics”), and (VU6) mafic and felsic tuffs. The northwards-younging SCU rocks are discussed as a single unit as individual beds do not define laterally coherent subunits as within the VU (Fig. 4). The relative age and stratigraphic position the SCU with respect to the VU will be discussed later.

(VU1) *The felsic volcaniclastics* are at its base composed of fine volcanic sandstones ("tuffs"; Fig. 4). These are followed by volcanic conglomerates/breccias ("lapillistones") covered by coarse tuffs (Fig. 3a), both of which are interbedded with more fine tuffs. The beds in this unit are relatively well sorted. S_1 is strong in the fine tuffs.

(VU2*) The intermediate volcaniclastics* contain two distinguishable types of strata: (a) sandy tuff with few lapillis and gradual variations in grain size leading to diffuse strata boundaries, and (b) graded lapillistone interlayered with sandy tuff, including some cobble-sized fragments of porphyritic lavas (Figs. 3b & 4). Some of the lapillis are strongly angular. Both types are rich in biotite and show strong S_1.

(VU3) *The coherent felsic plagioclase porphyrys* contain feldspar phenocrysts of variable sizes (typically 1-3 mm in diameter, Figs. 3c & 4). A weak S_1 schistosity is observed, and networks of hydrothermal veins are abundant.

(VU4)*The ur-pl porphyrys* envelope the subunits VU5 and VU6 (Figs. 3d & 4). They contain abundant c. 1-3 mm phenocrysts of uralite and/or plagioclase in fine-grained matrix. In the northern part of this unit, uralite phenocrysts are more common, while plagioclase phenocrysts gradually become more dominant toward the south. S_1 is fairly weak in the northern part of the subunit but becomes strong towards the south. Both dextral and sinistral sigma clasts and S-C structures are observed in the southern part of the unit, but most of the observed indicators show sinistral shear.

(VU5) *The southern volcaniclastics* are exposed within two elongated areas, separated by the subunit VU6 (Figs. 3e & 4). VU5 consists mainly of volcanic sandstones, pebbly sandstones, and conglomerates, but some tuff breccias rich in angular clasts are also observed. Weak S_1 is present. As is typical for other VU rocks, ripples and erosion surfaces in this subunit show southward top-of-strata, but only in the exposures that are located north of VU6 (Figs. 3e & 4). South of VU6, the VU5 rocks show northward top-of-strata. S_1 is weak.

(VU6) *The mafic and felsic tuffs* consist of alternating fine-grained mafic and felsic layers. The felsic material often occurs as lenses within the mafic material (Fig. 3f). F_1 tight to isoclinal folds with steep axial planes and c. 40° eastward plunging fold axes are observed (Fig. 3f). Close to the Siitama batholith, F_2 refolds the F_1 folds into open to closed folds with fold axes plunging c. 60° toward the SE-ESE (Fig. 4).

(SCU) *The SCU* (Figs. 3g-l) shows laterally varying layer thicknesses in an E-W direction so that the conglomerates, the sandstones and the mudstones define interfingered lensoid shapes on the geological map (Fig. 4). The grain size variations define rhythmic ('cyclic') patterns at the map scale, with overall fining-upward sequences (younging towards north). The only folds that can be observed are very local, tight, asymmetric (dextral) folds in the southern part of the metasiliciclastic unit (Fig. 4). These folds show W-E to NW-SE striking, steeply dipping axial planes and roughly 40° east- to southeastwards plunging fold axes.

Sulphide-bearing schists appear in three exposures within the SCU (Figs. 3j & 4). Two of the exposures occur in the central part of the mapping area, close to the contact with the Siitama batholith and the VU, and one exposure is a thin horizon in the northwest. In addition, sulphide schist are also found within the Siitama batholith (Fig. 4). The sulphide schists are often extensively weathered and eroded, and have rusty outcrop surfaces. The bedding or other structures are not easily observable, but a few coarser-grained sandstone lenses are distinguishable in places. S_1 is subparallel to S_0 (where visible). The sulphide mineralisation consists mainly of small amounts of disseminated pyrite and chalcopyrite visible to the naked eye, and of secondary mineralisation (mainly haematite) identifiable in the fractures in thin section (Figs. 3k & l). In thin section, the S_1 is strongly developed, defined by elongate micas and opaque minerals (Figs. 3k & l). It is notable that the opaque minerals, presumably pyrite/chalcopyrite, and haematite, are present both within the S_1 and within the fractures cross-cutting it. The economic potential of the sulphide schists within the study area has not been assessed, but the grade seems to be low.

Interpretation

Structure

The observed S_1 schistosities are relatively constant throughout the area (Fig. 4). S_1 is generally striking E-W and (sub)parallel to the bedding S_0. S_1 is interpreted to represent the main deformation phase D_1 (i.e. main inversion and basin closure), which resulted in the large-scale folding and the formation of the TSB syncline. The intensity of the S1 schistosity is directly dependent on the lithotype: it is best formed in the mudstones but only weak in the sandstones and many of the coherent porphyritic metavolcanics. In the absence of clear signs of significant lateral movement (shearing) in most parts of the mapping area, the dominantly E-W strikes of the S_1 would imply approximately N-S shortening during D_1, in accordance with previous works (e.g. Kähkönen 1989; Nironen 1989a). The appearance of dominantly sinistral kinematic markers toward the south, affecting also the northernmost edge of the Siitama batholiths, suggests that the continuation of the Tampere shear zone (TSZ) exists in this area, and that the shear sense along the TSZ was sinistral, at least at the time of the emplacement of the batholith (c. 1.88-1.87 Ga).

S_2 is locally observed, and it constantly strikes at an angle of c. 40-50° counter-clockwise from S_1. S_2 is usually, but not always, observed in the mudstones, where it is seen to crenulate S_1. S_2 is interpreted to represent a D_2 deformation phase separate from and younger than S_1. Like S_1, S_2 is not seen to be associated with pervasive lateral shear in the field, so that the dominantly NE-SW strike of the S_2 suggests an approximately NW-SE oriented compression during D_2. The D_2 is probably unrelated to the sinistral TSZ shearing, as a NW-SE compression would have resulted in dextral shearing along the TSZ.

The polarity observations imply a previously unknown F_1 syncline, 'the Pohjala syncline', in the VU (Figs. 4 & 5). The tightly folded rocks of subunit VU6 form the core of the syncline. The c. 40° eastward plunge of the F_1 fold axes in VU6 is interpreted to be representative for the entire syncline. The Pohjala syncline is best defined by the subunit VU5 that shows opposite bedding polarities on the north vs. south sides of the VU6 (Figs. 4 & 5). The rest of the subunits (VU1-VU4) form the northern limb of the Pohjala syncline (a narrow zone of subunit VU4 is also present in the southern limb). The c. 40° eastward plunge of Pohjala syncline is interpreted to at least partly result from the intrusion of the Siitama batholith. In the hinge zone of the Pohjala syncline (in VU6), the F_2 folding event is seen to refold the isoclinal F_1 folds. The F_2 folds are open to closed folds with hinge lines plunging c. 60° toward the SE-ESE. They are interpreted to be related to the sinistral shearing along the TSZ.

In the SCU, north of the VU, both the lithology and the polarity indicators abruptly change (Fig. 4): igneous rocks are present only as relatively thin sills/dykes and, except at one location close to the VU/SCU transition, the SCU rocks consistently show northward top of strata. The SCU rocks also show mostly northward dipping S_0. The age of the dykes/sills is unknown, but they show S_1 schistosities. The tight, asymmetric folds observed in the southern part of the SCU are interpreted to be F_1 folds. There is a possibility that the intrusion of the Siitama batholith has caused the local folding. However, due to the similarity between these folds and the F_1 folds within the Pohjala syncline (similar tight to isoclinal folding with moderately eastward-plunging hinge lines), we interpret both folds to have formed during the main deformation (folding) phase. It is unclear whether the dextral asymmetry of the F_1 folds at the bottom of the SCU reflects a relative movement of the north-side-up, or whether the folds are parasitic folds of a larger fold within the metasiliciclastic unit. Because no sinistral F_1 folds have been found (corresponding the other hypothetical limb of a larger fold), and because the folds are only found close to an inferred fault zone (see below) we tentatively prefer the interpretation of these F_1 folds as shear folds indicating north-side-up reverse movement.

A discontinuity plane is interpreted to offset the SCU subunits (Fig. 4). The inferred fault has an apparent dextral kinematics and bends into parallelism with the S_0 in the southern part of the mapped metasiliciclastic unit (Figs. 4 & 5). The age of the inferred fault is uncertain. It may, therefore, represent either a late dextral fault zone, formed as a response to D_2 with c. NW-SE compression or alternatively it might form a part of an imbricate thrust system formed during D_1 (the dextral offset therefore being apparent).

The most extensive sulphide schist occurrences in the area are found in the lowest parts of the SCU near the contact with the VU (Figs. 4 & 5). The sulphide mineralisation is interpreted to have occurred in two phases. The first mineralisation phase occurs within the S_1 (Figs. 3k & l). Therefore, the mineralisation is interpreted to be genetically linked to the formation of S_1 and to the closure of the basin. The sulphide-bearing hydrothermal fluids from which the minerals precipitated probably sourced from deeper within the basin. The second phase occurred during a brittle deformation event and also suggests hydrothermal fluid activity within the area. There is no indication in the thin sections that the S_1 –related mineralisations were remobilised during this event. A possible source for this second-phase fluids is the Siitama batholith. However, sulphide schist blocks have been found within the batholith, so that the mineralisation within the schist must, therefore, be older than the intrusion (1.88-1.87 Ga). Sulphide schist has also been observed north of the study area, kilometres away from the batholith, further suggesting a remobilisation of sulphides by another mechanism than magmatic fluids. Finally, not all the schists and none of the other rock types are sulphidised, which would be expected with a near-by magmatic source.

Architecture

The SCU and VU can be reasonably correlated with the Karppi turbidites and the Pohjala volcanics, respectively, east of the mapping area (Fig. 1a; see also Seitsaari, 1951). We also correlate the SCU with the turbidites of the Myllyniemi Fm. (Fig. 1; Kähkönen 1999) also typically located in the southern limb of the main TSB syncline (Figs. 1b, 2; Kähkönen 1989; Nironen 1989a). In accordance with previous works, we interpret the interfingered metasilicilastic rocks of the SCU to have been formed in a submarine turbidite fan coevally with the other Myllyniemi-type sedimentary rocks at c. 1.92-1.90 Ga (Fig. 6). At least five fining-upward cycles at a 100-metre scale are observed in the mapped part of this unit, suggesting stepwise basin subsidence/sea level transgression (Fig. 4). Alternatively, the apparent repetition of the cycles might be caused by a development of an imbricate system within the SCU.

The architecture of the VU is simpler than that of the SCU, assuming that the porphyries of VU4 are completely extrusive and not sills. The tuffs, lapillistones, and porphyries (VU1-VU4) are overlain by the relatively thin volcaniclastic VU5. The ripples in the sandstones of VU5 are consistent with erosion and redeposition within a dynamic volcanic environment (Fig. 3e). The youngest rocks within the VU are the fine VU6 tuffs in the core of the Pohjala syncline (Fig. 3f). The rheological differences during deformation between the mafic and the felsic material in VU6 are interpreted to be responsible for the break-up of the felsic material into fragments, whereas the mafic material behaved more ductilely.

The relative age of the VU with respect to the SCU is not immediately obvious from the collected data. The age relationship of the units has consequences to the resulting geological model: this is discussed in the following chapter.

Discussion

Geological model

The mapping reveals a ‘double-syncline’ (Figs. 4 & 5): the Pohjala syncline within the VU in the south, and the larger TSB main syncline system in the north (only the metasiliciclastics-dominated southern limb of which extends into the mapping area). However, no anticline has been observed between the two synclines, and the transition from one syncline/unit to another (and from one bed polarity trend to another) is sharp. The single southward top-of-strata observation within the SCU close to the VU/SCU contact may represent remnants of an anticline, but this is very local as elsewhere along the contact the SCU top-of-strata indicators are systematically northward. This indicates that faulting must be involved and is responsible for the juxtaposition and the present configuration of the units. No such shear or fault zone is directly observed in the VU/SCU contact zone (however, the contact itself is not exposed). The primary structures are often very well preserved, even right next to the inferred contact zone, and the lack of asymmetric kinematic markers at outcrop suggest coaxial rather than shear deformation. The only possible asymmetric kinematic markers related to the inferred fault/shear zone are found in the mudstones near the VU/SCU contact: the asymmetric F_1 folds could be tentatively interpreted as shear folds indicating north-side-up reverse movement. The absence of obvious fault or shear zone indicators in the vicinity of the contact zone does not, however, as such contradict the hypothesis for faulting. Many examples exist worldwide of simple shear (non-coaxial strain) being strongly partitioned into narrow zones that accommodate large amounts of movement. For example, the Glencoul thrust in NW Scotland forms a part of a thin-skinned thrust system that accommodates up to tens of kilometres of transport along a mylonitic (non-coaxial) thrust zone that is only from some decimetres to up to some metres in thickness, while the strain directly below the shear zone is mostly coaxial (e.g. Butler 1984; Law 1987; Law *et al*. 2010).

The age relationship between VU and SCU is obscure: the polarity indicators and the lithologies and, therefore, the relative ages of the units cannot be systematically carried over from one unit to the other. However, if the asymmetry of the F1 folds observed close to the VU/SCU contact reflects north-side-up kinematics, then the SCU is older than the VU. This interpretation is supported the stratigraphic correlation with dated units elsewhere within the TSB. The VU seems to occupy an approximately similar stratigraphic position as the Tohloppi-Kiviranta-Sorila volcanics further west, whereas the Myllyniemi turbidites, presently north of the Tohloppi volcanics, can be correlated with the SCU (Kähkönen 1994; Fig. 1b). The depositional age of the Myllyniemi Fm. has been determined to 1.92-1.90 Ga while the Tohloppi-Kiviranta-Sorila volcanics are younger. Based on this implications that the VU is younger than the SCU, propose the following geological model for the studied area (Fig. 7).

1) The SCU was deposited, like other parts of the Myllyniemi Fm, mainly on a margin of a rifted microcontinent at c. 1.92-1.90 Ga, with the rift-related Haveri-type volcanics partly at the base (Figs. 6 & 7a). The lobate architecture of the SCU results from deposition largely on the microcontinental slope during continuing but stepwise basin subsidence (Fig. 6; see also Kähkönen 1999).

2) The onset of northward subduction and related arc-type volcanism at c 1.90 Ga caused a change to volcanism-dominated deposition in the TSB for the period of c. 1.90-1.89 Ga. In our study area, the volcanism resulted first in the deposition of the felsic and intermediate tuffs (VU1 and VU2), followed by the pl- and the ur-pl porphyrys (VU3 and VU4), the southern volcaniclastics (VU5), and finally the mafic to felsic tuffs (VU6).

3) During the continuing subduction basin inversion initiates with N-S compression (the local D_1 event; Fig. 7b). Some of the extensional faults are reactivated as (blind) reverse faults, leading to open folding of the VU and SCU. This stage of local “thick-skinned” deformation is needed to produce the original Pohjala syncline; a purely thin-skinned thrusting of sub-horizontal sedimentary packages on top of each other would probably have only resulted in repetition of units, without significant folding of the units in the footwall of the thrust.

4) As the basin closure progresses, the normal fault inversion cannot accommodate the increasing amount of shortening, and a southward-propagating “thin-skinned” thrust system develops (Fig. 7c). Where the thick-skinned shortening is accommodated at this point is not inferable from our data. The thrust planes localise approximately layer-parallel and break towards the surface when they meet the buried basement highs defined by the faulted and partly inverted blocks. The thrust system juxtaposes different geological units, including the observed southward-younging and northward-younging units. The earlier

anticlines are mostly destroyed as they are thrusted upwards and subsequently eroded. At least one major thrust is active within the VMB: this fault will later develop into the Tampere shear zone (TSZ; see also Nironen 1989a). The details of the development of TSZ are outside the scope of this study, but the TSZ thrust helps to accommodate the overall shortening and tightens the Pohjala syncline.

5) Continuing shortening leads to a tightening of the folds and in the rotation of the bedding and the thrust faults into an upright position (Fig. 7d). In their steeper position, the thrust faults would occupy a position that is mechanically unfavourable for reverse movements. Lateral (shear) movements along these previous thrust fault planes is more likely at this stage, the sense of shear possibly being mostly sinistral based on the field observations. However, bedding-perpendicular coaxial (pure) shear while the beds were in an upright position probably accommodate some shortening, so that the S_1 probably developed latest at this stage. At depth, the layer-parallel thrusts are folded together with the rock units that host them.

6) Latest at the time of the intrusion of the Siitama batholith c. 1.88-1.87 Ga, the sinistral lateral kinematics in this part of the Tampere shear zone is established and the structures have reached their final subvertical orientations (Fig. 7e).

7) The second deformation phase D2, with compression from c. SSE-NNW crenulates the S1 schistosities, and leads to localised dextral faulting within the metasiliciclastic unit (the curved fault, Figs. 4 & 5).

The bulk of the shortening is therefore accommodated partly by folding, partly by the thrusts, and partly by the bedding-perpendicular shortening (probably including volume change and compaction). The minimum amount of shortening across the VU can be calculated, on the basis of the folding of the VU, to a minimum of c. 50%. This shortening estimate cannot be directly extrapolated to the scale of the TSB, because VU-type folding is not at present identified in the northern parts of the belt. On the other hand, the interpreted overall geometry of the TSB (Fig. 2) and the implications of the structural model presented above suggest a minimum shortening of a similar order of magnitude. The estimate does not consider volume change, or account for the unknown total number of thrusts within the TSB. The possible existence of additional thrusts and/or imbricate/duplex systems within the SCU would mean that the total shortening was notably larger than 50%.

The model largely agrees with previously published literature in terms of the overall temporal and spatial development of the basin. The development of early thrusts and their subsequent rotation and folding at a large scale is inferred, confirming the interpretation of (Nironen 1989a). However, the model gives a more detailed suggestion for the structural development and shortening of the TSB that might explain some of the observed problems within the TSB (e.g. Nironen 1989a). Furthermore, contrary to Nironen (1989a), the implied main thrusting direction, at least in the southern margin of the TSB, is toward the south. A northward-verging thrust system cannot explain the observed structural geometries and the inferred age relationships; however, if the VU is older than the SCU, a northward-verging thrust system is possible. Northward structural vergences within and at the northern margin of the VMB are consistent with our model, and the model in fact requires that the Vammala area is uplifted (or a subduction complex/accretionary wedge develops) at an early stage of the basin inversion. Tampere are would, effectively, have formed a backstop to the developing Vammala wedge/complex.

The implications to the sulphide mineralisation

The sulphide mineralisation seems to be a result of a combination of sedimentary processes and hydrothermal activity (remobilisation) along restricted zones within the TSB. In thin section, the sulphide schist displays iron oxide and sulphide mineralisation both within the schistosity, and along the second-order fractures (Figs. 3k & l). The most prominent sulphide schist exposures within the study area are located close to the VU/SCU contact, where the presence of an early thrust is implied in our model. This spatial association suggests a genetic relationship between the localisation of the thrust fault, the occurrence of the schistosity-parallel mineralisation, and the localisation of the mineralised second-order fractures. The model suggests that the first mineralisation phase occurred at model stage 5) when hydrothermal, mineralised fluids moved within and close to the old thrust plane. The ore minerals were trapped within the developing S_1 schistosity close to the old thrust plane (Figs. 3k & l). The fluids probably sourced from within the lower parts of the basin, not exposed within the study area. If the base of the basin infill in our mapping area consists of similar VMS rocks than those that are interpreted to source at least the Haveri deposit, they might have served as a source for the dissolved metals in the hydrothermal fluids. Another possible source for the fluids is magmatic, but the nearest intrusion, the Siitama batholith, is younger than the sulphidisation (evidenced by the presence of sulphide schist xenoliths within the intrusion). Some of the mineralisation was remobilised later, or there was a new pulse of mineralised fluids, as evidenced by the haematite- and sulphide-filled second-order fractures (Figs. 3k & l). The age of the fractures is unknown but they localised within the inferred palaeothrust after the main schistosity within the thrust had formed, and may reflect later strike-slip movements inferred by our model. The results imply that presently subvertical mineralised fault zones may have originally been more gently dipping, and that they may not necessarily have sourced their minerals from great depths (i.e. from deep within the basement).

If the sulphide schists within the TSB are related to early thrusts, the presence of sulphide schists might help in deducing the structural geometries and the basin closure processes elsewhere within the basin, and possibly aid mineral exploration in the area. For example, the Kutemajärvi and Haveri deposits are at least partly fault-controlled, and both deposits are hosted by schists (e.g. Nironen 1994; Eilu *et al.* 2003). Furthermore, an extensive sulphide schist horizon outcrops just north of the mapped area, possibly indicating a presence of a prominent early thrust with similar mineralisation. A minor sulphide schist lens is also found in the northeastern part of the mapping area, implying that a minor thrust might exist here, possibly related to an unconfirmed imbricate system (Fig. 5).

Summary

- The detailed structure of a part of the Palaeoproterozoic, well preserved Tampere basin is described.
- The observed architecture and the structures of the volcanosedimentary rocks within the southeastern Tampere basin imply a presence of hitherto unrecognised palaeothrusts within the basin. These thrusts played an important role in accommodating the overall shortening during basin closure.

- We propose a conceptual tectonic model that implies a transition from a normal fault inversion-type crustal shortening, to locally ‘thin-skinned’ accommodation of shortening as the basin closure continued.
- The palaeothrusts were also key in the localisation of the fracture zones that transported and trapped sulphide-bearing hydrothermal fluids, as the sulphide mineralisations are spatially linked to the thrusts. The proposed tectonic model correlates the structural geometries observed in the field and the occurrence of the sulphide-bearing fractured schists.

Acknowledgements

This study was funded by a research grant from K. H. Renlunds Stiftelse, which is gratefully acknowledged. Reviewers, editor…

References

Allen, R. L., Weihed, P. & the Global VHMS Research Project team 2002. Global comparison of volcanic-associated massive sulphide districts. In: Blundell, D. J., Neubauer, F. & von Quadt, A. (eds) T*he Timing and Location of Major Ore Deposits in an Evolving Orogen*. Geological Society, London, Special Publications, **204**, 13-37.

Butler, R. W. H. 1984. Structural evolution of the Moine thrust belt between Loch More and Glendhu, Sutherland. *Scottish Journal of Geology*, **20**, 161-179.

Claesson, S., Huhma, H., Kinny, P. D. & Williams, I. S. 1993. Svecofennian detrital zircon ages – implications for the Precambrian evolution of the Baltic Shield. *Precambrian Research,* **68**, 231-240.

Eilu, P., Sorjonen-Ward, P., Nurmi, P. & Niiranen, T. 2003. A review of gold mineralization styles in Finland. *Economic Geology*, **98**, 1329-1353.

Gaál G. & Gorbatschev R. 1987. An outline of the Precambrian evolution of the Baltic Shield. In: Gaál G. & Gorbatschev R. (eds) *Precambrian Geology and Evolution of the Central Baltic Shield.* Precambrian Research, **35**, 15-52.

Huhma, H., Claesson, S., Kinny, P. D. & Williams, I. S. 1991. The growth of early Proterozoic crust: new evidence from Svecofennian detrital zircons. *Terra Nova,* **3**, 175-179.

Kähkönen, Y. 1987. Geochemistry and tectonomagmatic affinities of the metavolcanic rocks of the early Proterozoic Tampere Schist Belt, southern Finland. *Precambrian Research,* **35**, 295-311.

Kähkönen, Y. 1989. Geochemistry and petrology of the metavolcanic rocks of the early Proterozoic Tampere Schist Belt, southern Finland. *Geological Survey of Finland, Bulletin*, **345**, 104 p.

Kähkönen, Y. 1994. Shoshonitic and high-K metavolcanic rocks in the southern parts of the Paleoproterozoic Tampere Schist Belt, southern Finland: evidence for an evolved arc-type setting. *Geological Survey of Finland, Special Paper,* **19**, 101-115.

Kähkönen, Y. 1999. Stratigraphy of the central parts of the Palaeoproterozoic Tampere schist belt, southern Finland: review and revision. *Bulletin on the Geological Society of Finland,* **71**, 13-29.

Kähkönen, Y. 2005. Svecofennian supracrustal rocks. In: Lehtinen, M., Nurmi, P. & Rämö, T. (eds) T*he Precambrian Bedrock of Finland – Key to the evolution of the Fennoscandian Shield.* Elsevier B.V., Amsterdam, 343-406.

Kähkönen, Y., Huhma, H. 2012. Revised U-Pb zircon ages of supracrustal rocks of the Palaeoproterozoic Tampere Schist Belt, southern Finland. In: Kukkonen, I. *et al.* (eds) *Lithosphere 2012, Programme and extended abstracts.* Institute of Seismology, University of Helsinki, Report S-56, 132 p.

Kähkönen, Y., Huhma, H. & Aro, K. 1989. U-Pb zircon ages and Rb-Sr whole-rock isotope studies of early Proterozoic volcanic and plutonic rocks near Tampere, southern Finland. *Precambrian Research*, **45**, 27-43.

Kähkönen, Y., Huhma, H. & Mänttäri, I. 2004. TIMS and SIMS U-Pb zircon ages and Rb-Sr whole-rock isotope studies of early Proterozoic volcanic rocks near Tampere, southern

Finland. In: Mansfield, J. (ed) T*he 26th Nordic Geological Winter Meeting, Abstract Volume.* GFF, **126**, 25.

Kähkönen, Y. & Nironen, M. 1994. Supracrustal rocks around the Paleoproterozoic Haveri Au-Cu deposit, southern Finland: evolution from a spreading center to a volcanic arc environment. *Geological Survey of Finland, Special Paper,* **19**, 141–159.

Kilpeläinen, T., Korikovsky, S., Korsman, K.& Nironen, M. 1994. Tectono-metamorphic evolution in the Tampere-Vammala area. *Geological Survey of Finland, Guide,* **37**, 27-34.

Korsman, K., Koistinen, T., Kohonen, J., Wennerström, M., Ekdahl, E., Honkamo, M., Idman, H. & Pekkala, Y. (eds) 1997. *Bedrock Map of Finland 1:1000000*. Geological Survey of Finland.

Lahtinen, R.& Huhma, H. 1997. Isotopic and geochemical constraints on the evolution of the 1.93-1.79 Ga Svecofennian crust and mantle in Finland. *Precambrian Research,* **82**, 13-34.

Lahtinen, R., Huhma, H., Kähkönen, Y. & Mänttäri, I. 2009. Paleoproterozoic sediment recycling during multiphase orogenic evolution in Fennoscandia, the Tampere and Pirkanmaa belts, Finland. *Precambrian Research*, **174**, 310-336.

Lahtinen R., Korja A. & Nironen M. 2005. Palaeoproterozoic tectonic evolution. In: Lehtinen, M., Nurmi, P. A. & Rämö, O. T. (eds) P*recambrian Geology of Finland – Key to the Evolution of the Fennoscandian Shield.* Elsevier B.V., Amsterdam, 481-532.

Law, R. D. 1987. Heterogeneous deformation and quartz crystallographic transitions: natural examples from the Moine Thrust zone at the Stack of Glencoul, northern Assynt. *Journal of Structural Geology*, **9**, 819-833.

Law, R. D., Mainprice, D., Casey, M., Lloyd, G. E., Knipe, R. J., Cook, B.& Thigpen, J. R. 2010. Moine Thrust zone mylonites at the Stack of Glencoul: I – microstructures, strain and influence of recrystallization on quartz crystal fabric development. In: Law, R. D., Butler, R. W. H., Holdsworth, R. E., Krabbendam, M., Strachand, R. A. (eds) *Continental Tectonics and Mountain Building: The Legacy of Peach and Horne.* Geological Society of London, Special Publications, **335**, 543-577.

Lentz, D. R. 1998. Petrogenetic evolution of felsic volcanic sequences associated with Phanerozoic volcanic-hosted massive sulphide systems: the role of extensional geodynamics. *Ore Geology Reviews*, **12**, 289-327.

Mäkelä, K. 1980. Geochemistry and origin of Haveri and Kiipu, Proterozoic strata-bound volcanogenic gold-copper and zinc mineralizations from southwestern Finland. *Geological Survey of Finland, Bulletin,* **310**. 79 p.

Nguyen, P. T., Cox, S. F., Harris, L. B. & Powell, C. McA. 1998. Fault-valve behaviour in optimally oriented shear zones: an example at the Revenge gold mine, Kambalda, Western Australia. *Journal of Structural Geology*, **20**, 1625-1640.

Nironen, M. 1989a. The Tampere schist belt: structural style within an early Proterozoic volcanic arc system in southern Finland. *Precambrian Research*, **43**, 23-40.

Nironen, M. 1989b. Emplacement and structural setting of granitoids in the early Proterozoic Tampere and Savo schist belts, Finland - implications for contrasting crustal evolution. *Geological Survey of Finland, Bulletin,* **346**, 83 p.

Nironen, M. 1994. Structural control and (re)mobilization of the extinct Haveri Au-Cu deposit, southern Finland. *Bulletin on the Geological Society of Finland,* **66**, 39–44.

Nironen, M., Elliott, B. A. & Rämö, O. T. 2000. 1.88-1.87 Ga post-kinematic intrusions of the Central Finland Granitoid Complex: a shift from C-type to A-type magmatism during lithospheric convergence. *Lithos,* **53**, 37-58.

Ohmoto, H. 1996. Formation of volcanogenic massive sulphide deposits: the Kuroko perspective. *Ore Geology Reviews*, **10**, 135-177.

Ojakangas, R. W. 1986. An early Proterozoic metagraywacke-slate turbidite sequence: the Tampere schist belt, southwestern Finland. *Bulletin of the Geological Society of Finland,* **58**, 241-261.

Patchett, J. & Kouvo, O. 1986. Origin of continental crust of 1.9-1.7 Ga age: Nd isotopes and U-Pb zircon ages in the Svecokarelian terrain of South Finland. *Contributions to Mineralogy and Petrology,* **92**, 1-12.

Piessens, K., Muchez, Ph., Dewaele S., Boyce A., De Vos W., Sintubin, M., Debacker, T. N., Burke, E. A. J. & Viaene, W. 2002. Fluid flow, alteration and polysulphide mineralisation associated with a low-angle reverse shear zone in the Lower Palaeozoic of the Anglo-Brabant fold belt, Belgium. *Tectonophysics*, **348**, 73– 92.

Poutiainen, M. & Grönholm, P. 1996. Hydrothermal fluid evolution of the Palaeoproterozoic Kutemajärvi gold telluride deposit, Southwest Finland. *Economic Geology,* **91**, 1335–1353.

Rutland, R. W. R., Williams, I. S. & Korsman, K. 2004. Pre-1.91 Ga deformation and metamorphism in the Palaeoproterozoic Vammala Migmatite Belt, southern Finland, and implications for Svecofennian tectonics. *Bulletin of the Geological Society of Finland,* **76**, 93-140.

Seitsaari, J. 1951. The schist belt northeast of Tampere in Finland. *Bulletin de la Commission Géologique de Finlande*, **153**, 121 p.

Sibson, R. H., Robert, F. & Poulsen, K.H. 1988. High-angle reverse faults, fluid pressure cycling and mesothermal gold– quartz deposits. *Geology,* **16**, 551–555.

Simonen, A. 1953. Stratigraphy and sedimentation of the Svecofennidic early Archaean supracrustal rocks in southwestern Finland. *Bulletin de la Commission Géologique de Finlande*, **160**, 64 p.

Teagle, D. A. H., Norris, R. J. & Craw, D. 1990. Structural controls on gold-bearing quartz mineralization in a duplex thrust system, Hyde– Macreas Shear zone, Otago schist, New Zealand. *Economic Geology,* **85**, 1711– 1719.

Weihed, P., Arndt, N., Billström, K., Duchesne, J.-C., Eilu, P., Martinsson, O., Papunen, H. & Lahtinen, R. 2005. Precambrian geodynamics and ore formation: the Fennoscandian Shield. *Ore Geology Reviews,* **27**, 273-322.

Williams, I. S., Rutland, R. W. R. & Kousa, J. 2008. A regional 1.92 Ga tectonothermal episode in Ostrobothnia, Finland: Implications for models of Svecofennian accretion. *Precambrian Research,* **165**, 15-36.

Figures

Fig. 1. a) Simplified geological map of the Fennoscandian shield. Key: **1** Phanerozoic sedimentary cover <0.57 Ga; **2** Caledonian rocks 0.6-0.4 Ga; **3** Sveconorwegian rocks 1.25-0.9 Ga; **4** Anorogenic rapakivi granites 1.65-1.4 Ga; **5** Late-Svecofennian granites and migmatites 1.85-1.77 Ga; **6** Early Svecofennian pre- and synorogenic magmatic rocks 1.95-1.85 Ga; **7** Early Svecofennian supracrustal gneisses and migmatites 2.0-1.85 Ga; **8** Early Palaeoproterozoic metasupracrustal rocks 2.5-1.9 Ga; **9** Archaean 3.2-2.5 Ga; Modified from Korsman et al. (1997). b) Generalised geological map of the Tampere area. Key: H = Haveri Cu-Au deposit; K = Kutemajärvi gold deposit; M = Myllyniemi; T = Tohloppi; Ka = Karppi; P = Pohjala, TSZ = Tampere shear zone. The location of Fig. 2 is shown with a rectangle. Modified from Kähkönen (1994, 1999), grid coordinates YKJ.

Fig. 2. Overall structure of the eastern part of the central TSB (see Fig. 1 for location and for key). U-Pb zircon age data are indicated (in billions of years, see text for references). Figure compiled and modified from Nironen (1989a; the cross section, individual units not shown) and Kähkönen (1994, 1999; map section). Width of the view is c. 16 km, length c. 28 km. The location of the study area is shown with a rectangle.

Fig. 3. Representative photos of the various rock types in the subunits described in the text. The VU subunits VU1-VU6 are shown in Figs. 3a-f, the SCU in Figs. 3g-l. a) VU1, stratified felsic volcanic sandstone; b) VU2, stratified intermediate volcaniclastic sandstone and conglomerate, erosion surface between the fine and the coarse layers indicates southwards top-of-strata (stippled line); c) VU3, felsic plagioclase porphyry; d) VU4, ur-pl porphyry; e) VU5, sandstone within the 'southern' volcaniclastics, subvertical section, view toward W; this exposure is located north of the subunit VU6 and shows southward younging strata; f) VU6, mafic and felsic tuffs; note the tight folds (F_1) with moderately (30-40°) eastwards plunging fold axes; g-j) SCU rocks: g) stratified, in part graded sandstones-microconglomerates, top of strata to the north (graded bedding); h) sandstones (in part graded) with mica-rich mudstone layer, top-of-strata to north; note the well preserved soft-sediment structures in the sandy layer (left of centre of the photo), and the NE-SW striking S_2 schistosity crenulating the S_1 in the mudstone (right of the centre); i) non-sulphidized mudstone; j) sulphide-bearing mudstone/schist; k-l) photomicrograph of the sulphide-bearing schist, in plane-polarised light (k), and in cross-polarised light (l). The schistosity is

defined by brown mica. Note the abundant opaque minerals associated with the mica, and the secondary fractures mineralised with red haematite and opaques. The opaques are presumably mostly pyrite and chalcopyrite, observable in some hand samples. The non-sulphidized schists do not contain abundant opaque minerals in thin section.

Fig. 4. Geological map of the study area, with the interpreted fault/shear zones. See text for age references and discussion. The bedding (S_0) symbols are omitted for clarity; the bedding is normally subparallel to S_1 schistosity. See also Fig. 5.

Fig. 5. A 3D block diagram presenting the interpreted structural geometry of the study area. The legend is as in Fig. 4. The volcanic unit (VU) forms the "Pohjala syncline", defined by the opposite younging directions of the VU units. The VU is separated from the siliciclastic unit (SCU) by a fault, interpreted as an early (D_1) thrust fault (see text and Fig. 7). The second, curved, right-lateral strike slip fault offsetting the siliciclastic subunits is interpreted to have formed during a later deformation phase (D_2).

Fig. 6. Conceptual diagram of the interpreted depositional environment and the succession for the metasiliciclastic and metavolcanic rocks of the SCU and VU, respectively. The study area essentially represents a submarine (turbidite) fan close to submarine and/or island arc volcanism.

Fig. 7. Conceptual tectonic model for the (southern) Tampere basin, not to scale. The general crustal-scale tectonic evolution (from continental rift to a continental slope in Fig. 7a, to a subduction setting in Fig. 7b, and finally to a collisional setting in Fig. 7d) is not shown. The internal architecture of the SCU and VU illustrated in Fig. 6 are omitted for clarity. See text for a more detailed discussion. a) Deposition of the SCU sediments the SCU units are deposited on a rift marginal basin (turbidite fans on a continental slope). b) Subduction and associated volcanism initiates, and leads to basin inversion and a creation of an (intra-arc) basin at c. 1.89 Ga. The volcanic activity leads to the deposition of the VU (note that the entire volcanic package in the TSB is much thicker than inferred in the figure). Some of the extensional faults are reactivated as (blind) reverse faults, leading to open folding of the volcanic and turbiditic units along the southern margin of the basin. c) A southward-propagating thrust, rooting layer-parallel within the SCU, develops to accommodate further shortening of the TSB. Imbricate faults may form at this point within

the SCU (omitted from the model). Hydrothermal fluids sourcing from the base of the basin infill (that possibly contains Haveri-type VMS mineralisations) may start channelling into the thrust zone at this stage. Note that the northernmost thrust and the associated synclines (outside the study area) are hypothetical, the thrust only inferred due to the presence of sulphide schist horizons north of the study area. Within the Vammala basin, another thrust with an opposite thrust direction (S-side-up) develops at the southern margin of the basin (or possibly already during the previous stage). d) The continued shortening leads to a tightening of the folds and in the rotation of the thrust faults into an upright position. At depth, the thrusts may be folded together with the rock units that host them. S_1 starts to form, trapping the sulphides of the first mineralisation phase. At the end of this phase, further reverse movements along the old thrust planes are unlikely, but strike-slip deformation can be expected. Fracture zones develop in the palaeothrust planes, forming a trap to the secondary mineralisation within the fractures (see text). e) Basin closure and S_1 is finalised, and the Siitama batholith intrudes along the interpreted continuation of the TSZ.

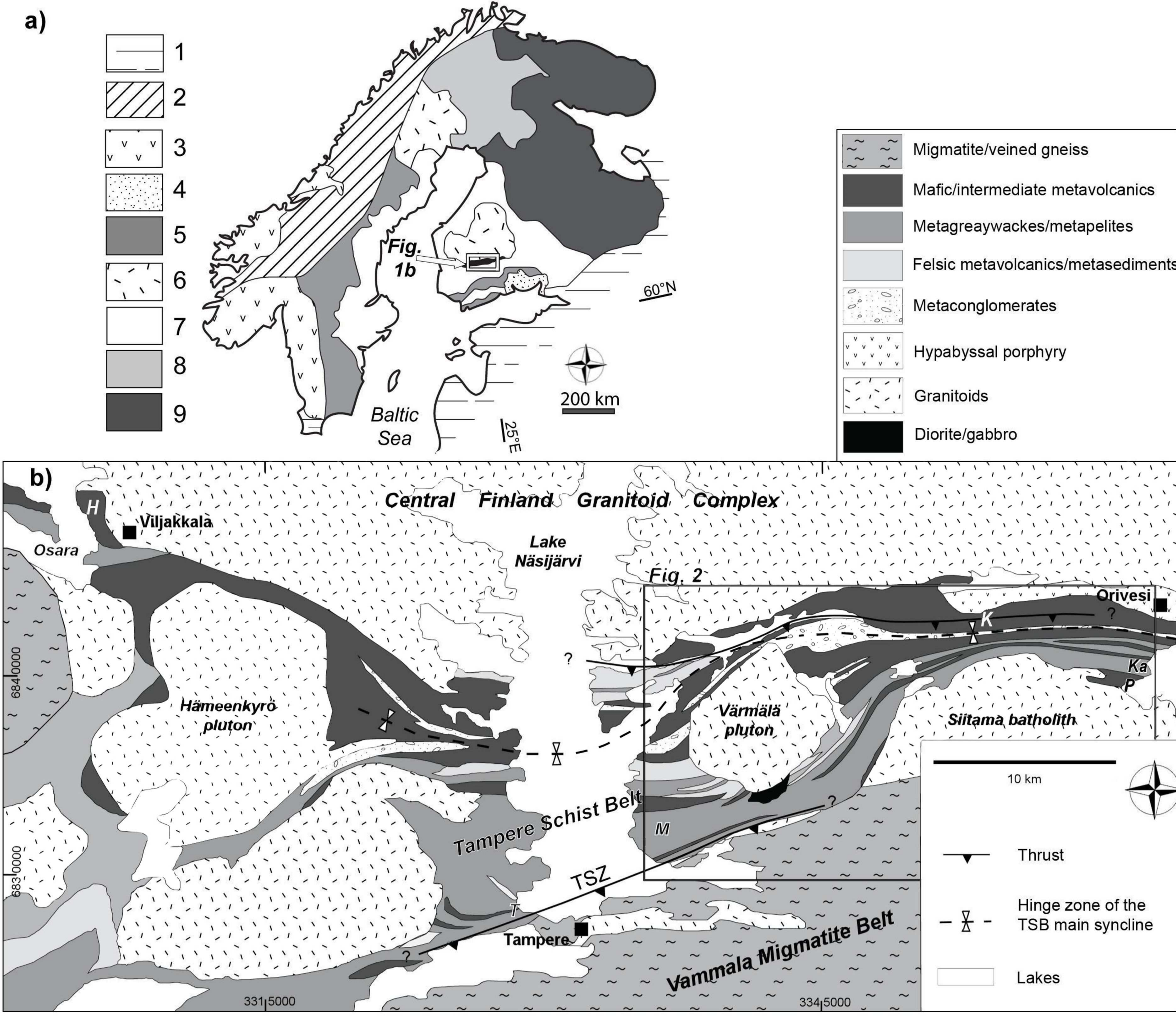
a)
1
2
3
4
5
6
7
8
9
Fig. 1b
60°N
25°E
200 km
Baltic Sea
Migmatite/veined gneiss
Mafic/intermediate metavolcanics
Metagreaywackes/metapelites
Felsic metavolcanics/metasediments
Metaconglomerates
Hypabyssal porphyry
Granitoids
Diorite/gabbro
b)
Central Finland Granitoid Complex
H
Viljakkala
Osara
Lake Näsijärvi
Fig. 2
Orivesi
K
Ka
P
Hämeenkyrö pluton
Värmälä pluton
Siitama batholith
10 km
Tampere Schist Belt
M
TSZ
T
Tampere
Vammala Migmatite Belt
Thrust
Hinge zone of the TSB main syncline
Lakes
6840000
6830000
3315000
3345000

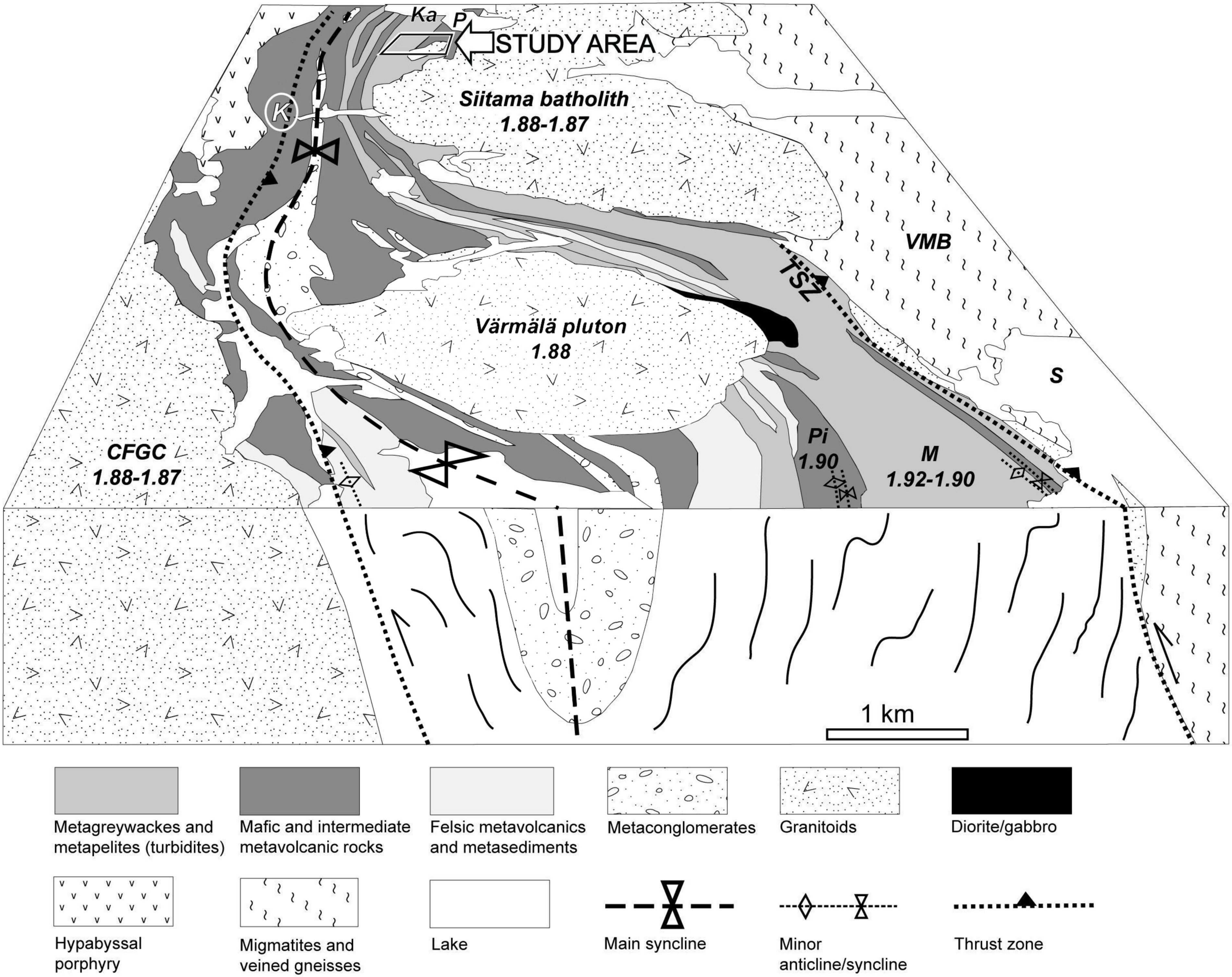
Ka
P
STUDY AREA
K
Siitama batholith
1.88-1.87
VMB
TSZ
Värmälä pluton
1.88
S
CFGC
1.88-1.87
Pi
1.90
M
1.92-1.90
1 km
Metagreywackes and metapelites (turbidites)
Mafic and intermediate metavolcanic rocks
Felsic metavolcanics and metasediments
Metaconglomerates
Granitoids
Diorite/gabbro
Hypabyssal porphyry
Migmatites and veined gneisses
Lake
Main syncline
Minor anticline/syncline
Thrust zone


a)
b)
c)
d)
e)
f)
g)
h)
i)
j)
k)
200 µm
l)
200 µm

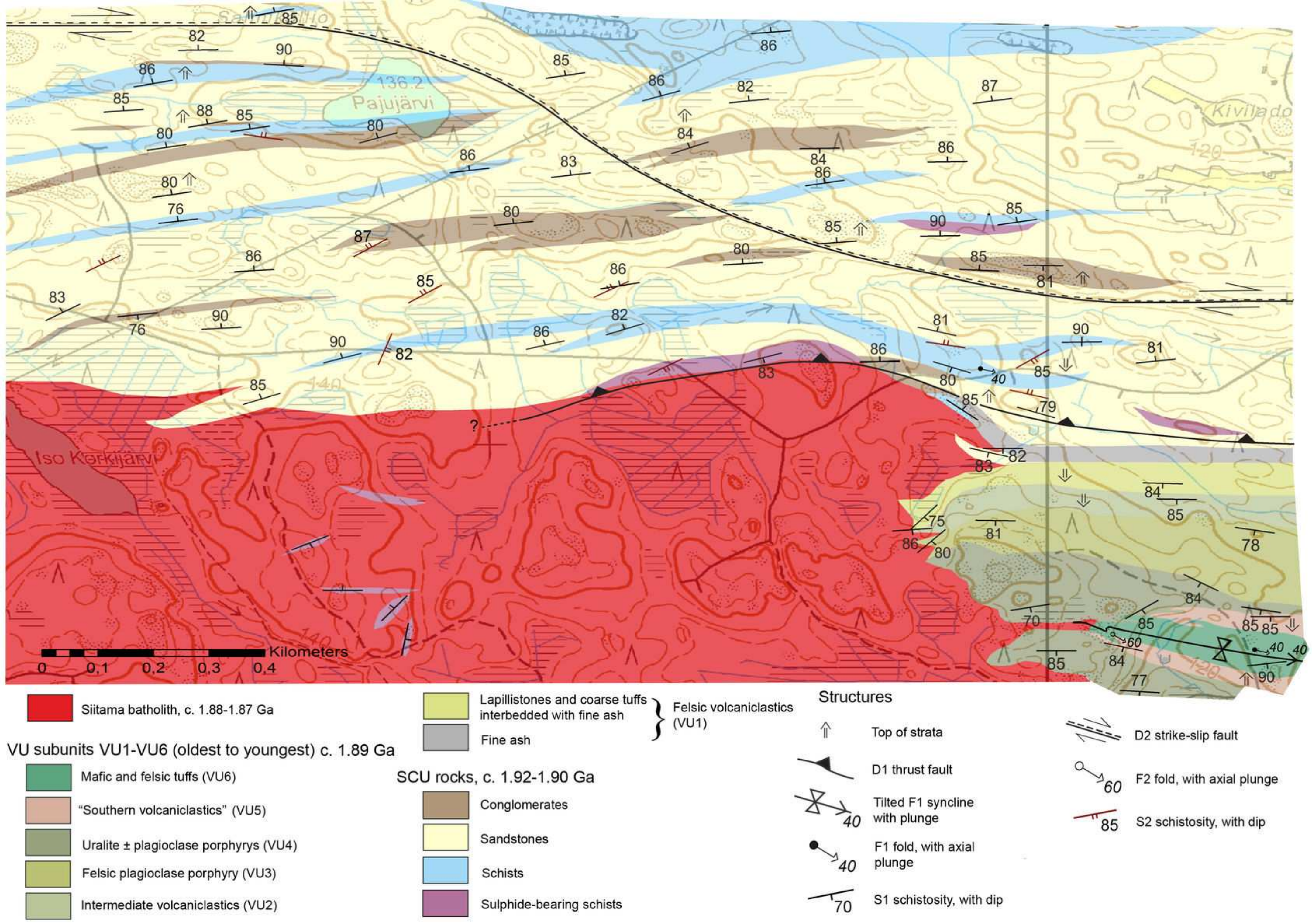

Pajujärvi
136.2
Iso Korkijärvi
Kilometers
0
0,1
0,2
0,3
0,4
Siitama batholith, c. 1.88-1.87 Ga
VU subunits VU1-VU6 (oldest to youngest) c. 1.89 Ga
Mafic and felsic tuffs (VU6)
"Southern volcaniclastics" (VU5)
Uralite ± plagioclase porphyrys (VU4)
Felsic plagioclase porphyry (VU3)
Intermediate volcaniclastics (VU2)
Lapillistones and coarse tuffs interbedded with fine ash
Fine ash
Felsic volcaniclastics (VU1)
SCU rocks, c. 1.92-1.90 Ga
Conglomerates
Sandstones
Schists
Sulphide-bearing schists
Structures
Top of strata
D1 thrust fault
Tilted F1 syncline with plunge
40
F1 fold, with axial plunge
40
S1 schistosity, with dip
70
D2 strike-slip fault
F2 fold, with axial plunge
60
S2 schistosity, with dip
85

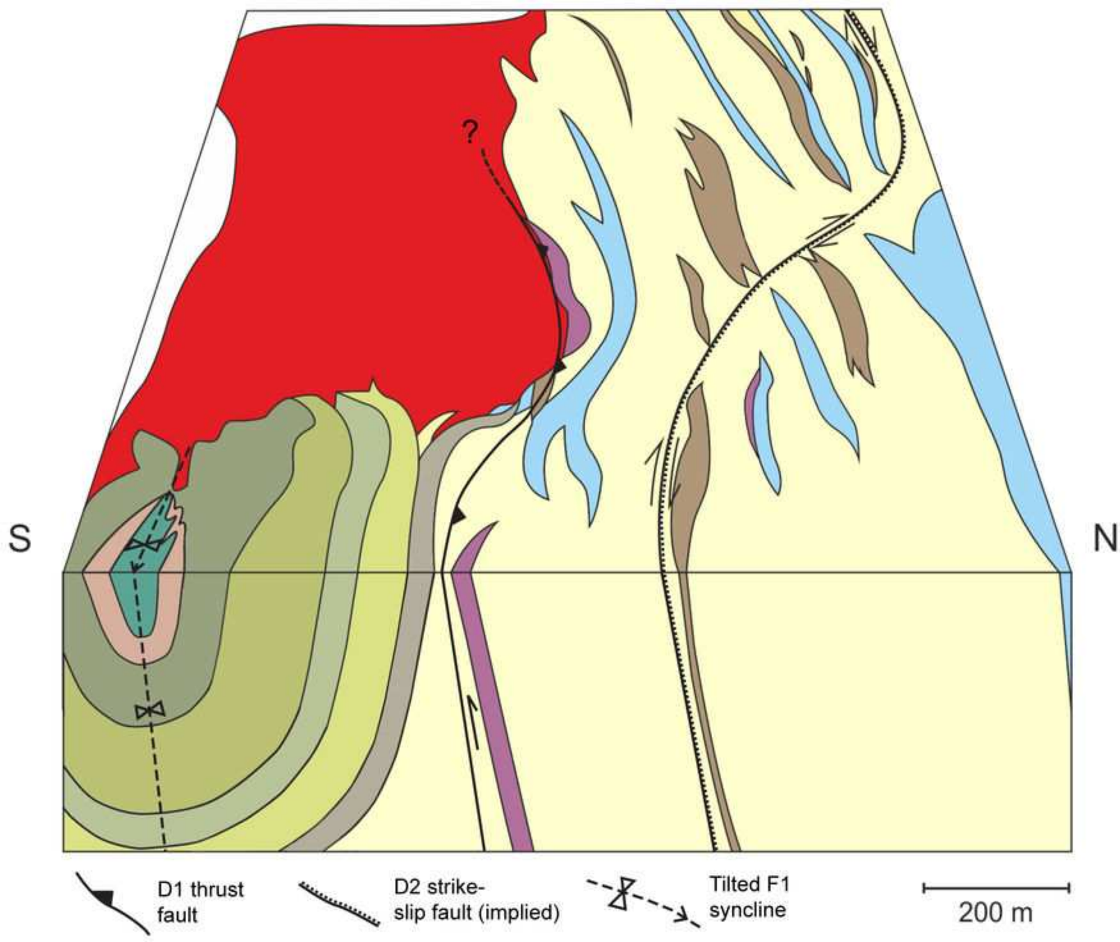

S
N
?
D1 thrust fault
D2 strike-slip fault (implied)
Tilted F1 syncline
200 m

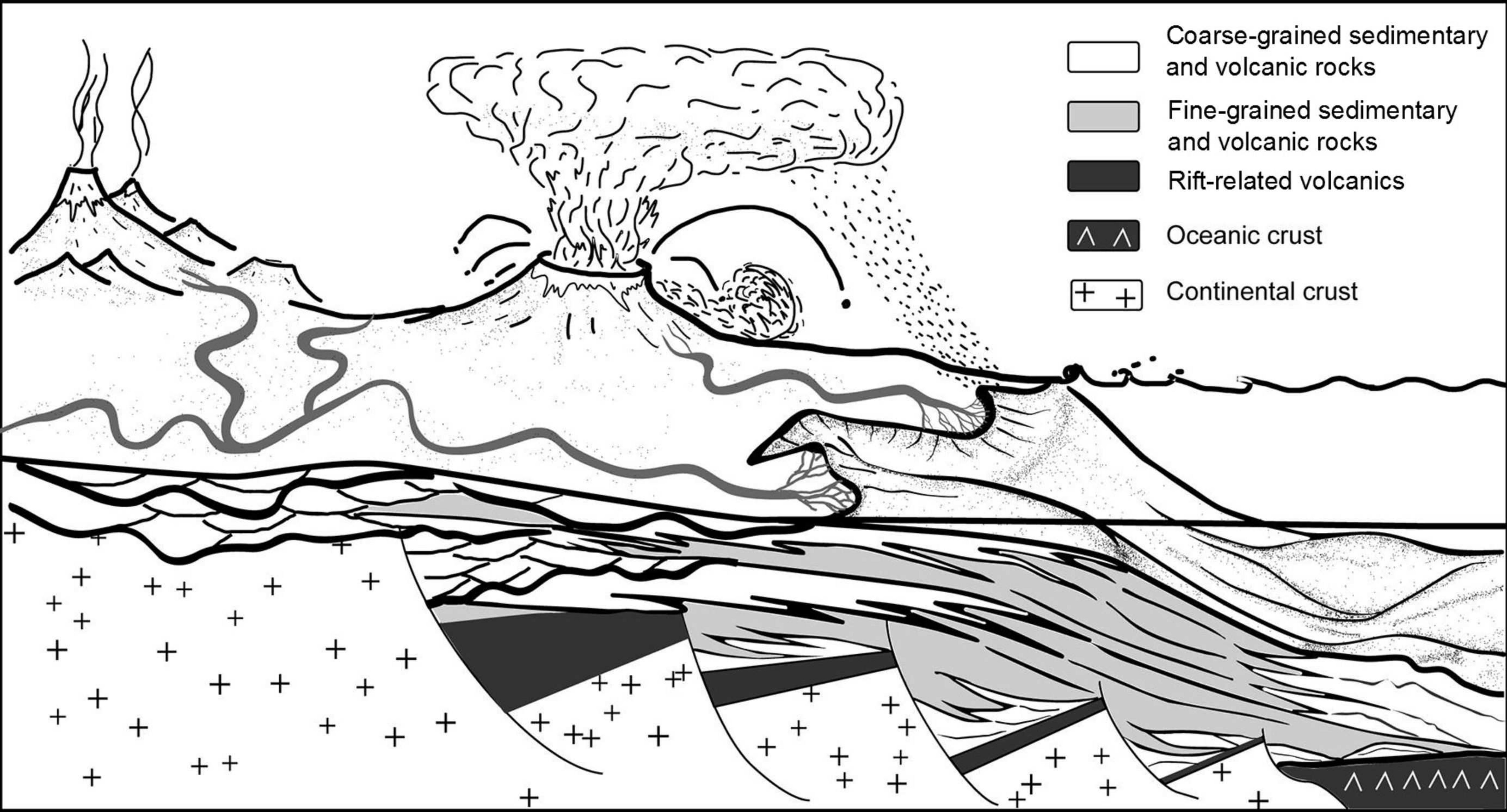
Coarse-grained sedimentary and volcanic rocks
Fine-grained sedimentary and volcanic rocks
Rift-related volcanics
Oceanic crust
Continental crust


a)
Continental rift/slope stage: deposition of SCU in an extensional basin/continental slope ~1.91-1.89 Ga
South
North
Possible basement high
Vammala basin
Tampere basin
SCU
Haveri-type basaltic volcanism at the base
Future inverted normal faults
b)
Onset of subduction, basin inversion, volcanism VU units deposited ~ 1.89-1.88 Ga
Vammala subduction complex developing in the south
Initial shortening by normal fault inversion
c)
Thickening of crust in Vammala area by unknown mechanism, but at least one major thrust active
Further shortening in Tampere basin by thin-skinned layer-parallel thrusting.
Basin closure stage ~1.88-.187 Ga
d)
S1 schistosity trends develop
Tightening of folds, rotation of faults; strike-slip shearing and faulting along earlier thrust zones provides channels for mineralising fluids
e)
TSZ
Pohjala syncline
Present erosion level
Siitama batholith
Study area
Final basin closure, intrusion of Siitama batholith.
Active fault
Inactive fault, or fault with minor activity
Major shear zone
Sinistral kinematics along a fault/shear zone